502 35100

量測原理與機工實驗

III. Flow Visualization

Instructor: Kuo-Long Pan
潘國隆

Department of Mechanical Engineering
National Taiwan University
May 25, 2011

1

Course Content of Lecture III

- Marker methods

For liquids (hydrodynamic)
- Surface marking
- Continuous dye injection (streakline marking)
- Particle tracing (pathline marking)
- Line marker generation (timeline marking)

For gases (aerodynamic)
- Surface marking
- Continuous smoke injection (streakline marking)
- Particle tracking (pathline marking)
- Line marker generation (timeline marking)

Ex. An undergraduate project

- Optical methods
  - Shadowgraphy
  - Schlieren
  - Interferometry
  - Holograhpy

- Other methods
  - Wall trace methods
  - Self-visible

References (major):

R. J. Goldstein, *Fluid Mechanics Measurements*, Hemisphere, 1983
S. Tavoularis, *Measurement in Fluid Mechanics*, Cambridge Univ., 2005

2

Marker Methods for Liquids (Aerodynamic Flow Visualization)

	Speed range
▪ Tufts: surface tufts, in-flow tufts, streamers, tuft screen	0.1 m/s – M1
▪ Surface marking	
• Oil streaks/dots	20 m/s – M10
• Oil film	5 m/s – M6
• Sublimation	10 m/s – M2
• Temperature-sensitive paint	150 m/s – M6
▪ Continuous smoke injection (streakline marking)	0.1 m/s – M1

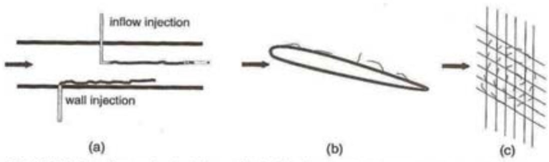

Figure 7.2. Simple flow-marker techniques: (a) dye injection through hypodermic tubes and wall taps; (b) use of tufts to identify flow separation over an airfoil; and (c) use of a tufts screen to visualize a wing-tip vortex.

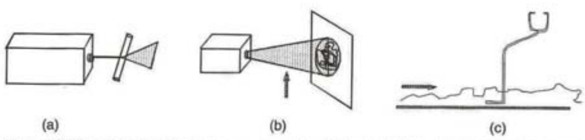

Figure 7.3. (a) Use of a cylindrical lense to produce a laser-light sheet; (b) simple shadowgraph by use of a slide projector; and (c) detection of turbulence by sound.

Photocopied from Tavoularis (2005)

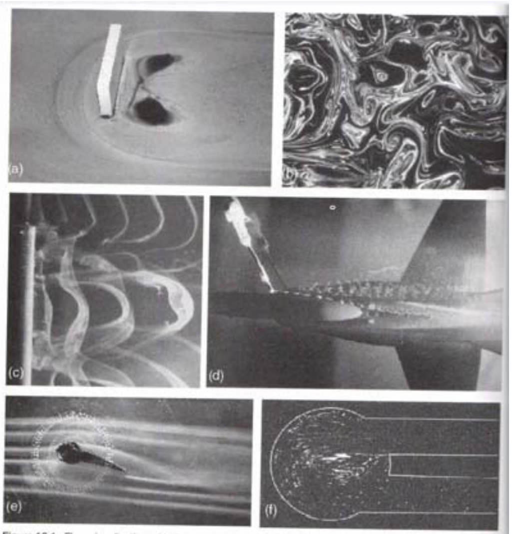

Figure 10.1. Flow visualization with the use of relatively simple marker techniques: (a) oil-streak visualization of flow adjacent to a plane surface with a bluff protrusion; the mixture consists of a suspension of 3 ml of graphite powder in 70 ml of penetrating oil (photograph by Sean Bailey); (b) laser-sheet visualization of fluorescent dye in a highly turbulent shear flow (photograph by Sebastien Marinau-Mes); (c) visualization of water flow past a cylinder with a step change in diameter by use of electrolytic precipitation of lead (photograph by Warren Dunn); (d) hydrogen-bubble visualization of the vortex produced by the leading-edge extension of a fighter aircraft model (photograph by Warren Dunn); (e) smoke-line (oil-mist) visualization of flow separation from an airfoil (photograph by Warren Dunn); and (f) visualization of pulsatile flow in a ventricular-assist-device model by use of laser-illuminated polysterene particles impregnated with a fluorescent dye (photograph by Jean-Baptiste Vergniaud).

Photocopied from Tavoularis (2005)

5

	Speed range
▪ Particle tracing (pathline marking): suspended solid markers, droplets, bubbles	1 – 20 m/s
▪ Line marker generation (timeline marking)	
• Smoke wire	0.3 – 8 m/s
• Sparks	2 m/s – M8
▪ Optical methods	
• Shadowgraph	70 m/s – M4
• Schlieren	2 m/s – M3
• Interferometry	70 m/s – M10

6

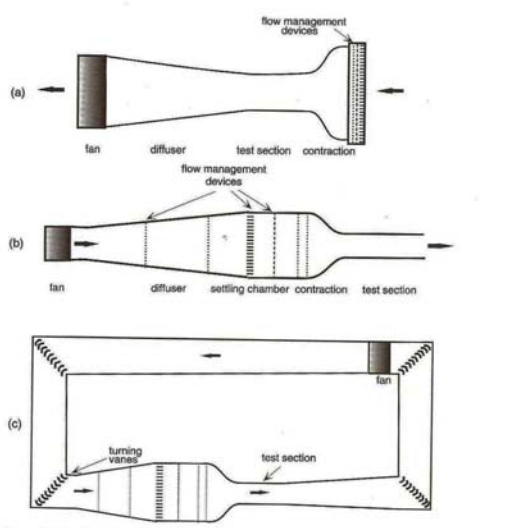

Figure 6.2. Sketches of representative low-speed wind tunnels: (a) suction tunnel, (b) blowdown tunnel, and (c) closed-circuit tunnel.

Photocopied from Tavoularis (2005)

7

Low-turbulence subsonic smoke tunnel (Notre Dame Aerospace Lab, copied from *Fluid Mechanics Measurements*, Goldstein, 1983)

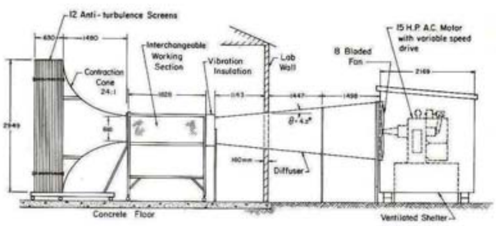

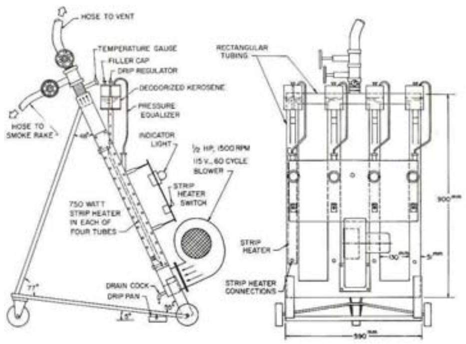

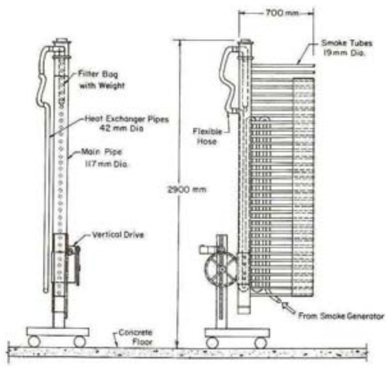

8

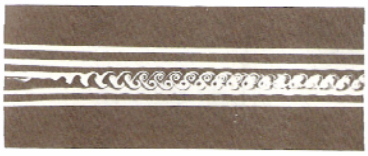

Figure 17 Flat plate of Fig. 16; $U_{\infty} = 8.5$ m/s and sound frequency of 0 Hz. *(Courtesy of University of Notre Dame.)*

Figure 21 Supersonic flow past a 5° half-angle wedge; Ma = 1.38. *(Courtesy of University of Notre Dame.)*

Smoke-tube application

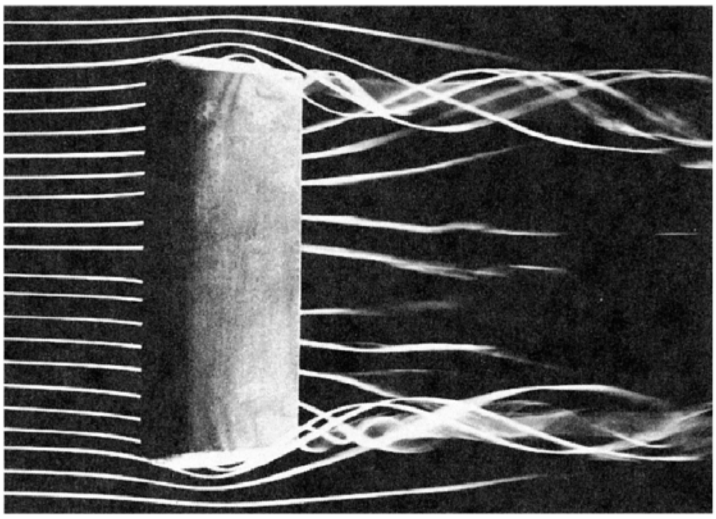

Figure 4.3 (p. 154)

Flow visualization of the complex three-dimensional flow past a model airfoil. (Copied from Munson et al., *Fundamentals of Fluid Mechanics*, 5th ed., 2005, Photograph by M. R. Head.)

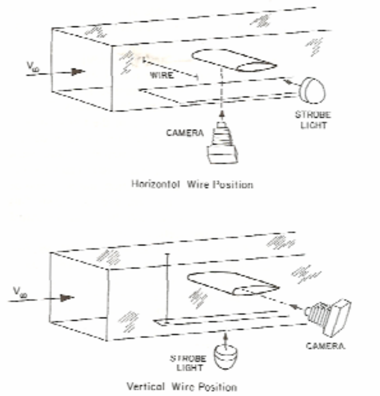

Figure 26 Wire, camera, and light locations for planform and profile views. *(Courtesy of T. J. Mueller and S. M. Batill, University of Notre Dame.)*

Figure 28 Smoke-wire visualization for a smooth NACA 66,-018 airfoil at an angle of attack of 12° and chord Reynolds number of 40,000. *(Courtesy of T. J. Mueller and S. M. Batill, University of Notre Dame.)*

Smoke-wire application

- Helium Bubble
  - Applicability in turbulence over smoke (diffusion)
  - Buoyancy neutral: soap filled with helium

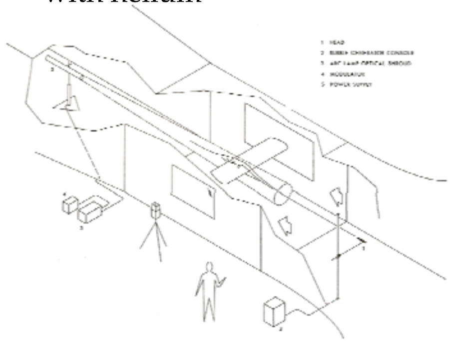

Figure 35 General arrangement of the helium-bubble visualization system in a wind tunnel [40]. *(Courtesy of Sage Action, Inc.)*

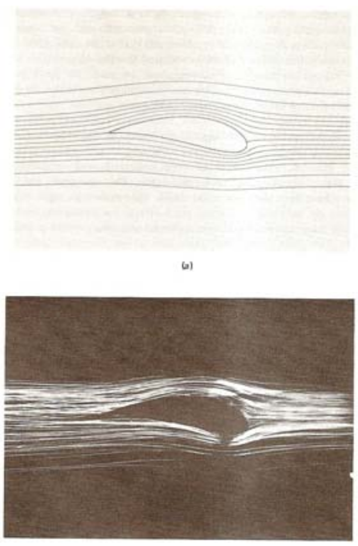

(a)

(b)

Figure 36 Comparison of the potential flow streamline pattern with a helium-bubble streak photograph for a two-dimensional Karman-Trefftz airfoil [40]. (a) Streamlines of potential flow field. (b) Streak photograph from wind-tunnel test (12). *(Courtesy of Sage Action, Inc.)*

Marker Methods for Liquids (Hydrodynamic Flow Visualization)

	Speed range
▪ Tufts: surface tufts, in-flow tufts, streamers, tuft screen	0.05 – 2 m/s
▪ Surface marking	
• Oil streaks/dots	0.5 – 4 m/s
• Oil film	0.1 – 25 m/s
• Electrolytic etching	0.01 – 0.1 m/s
▪ Continuous dye injection (streakline marking)	0.5 mm/s– 10 m/s

	Speed range
▪ Particle tracing (pathline marking): suspended solid markers, droplets, bubbles,	0.1 mm/s – 30 m/s
floating solid markers	0.5 mm/s – 5 m/s
▪ Line marker generation (timeline marking)	
• Hydrogen bubbles	5 mm/s– 10 m/s
• Thymol blue	< 0.1 mm/s
• Photochromic	< 0.1 mm/s
• Electrolytic precipitation	0.5 mm/s – 0.1 m/s

- Water tunnel
  - *Water tunnel*: usually closed loop, components as those of wind tunnels
  - *Water channel/flume*: with free surface
  - Specialized variations: stratified flow, low *Re*, matching refractive-index, cavitation …

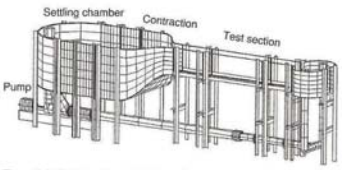

Figure 6.3. Sketch of a recirculating-flow water tunnel (drawing by Ben Kislich-Lemyre).

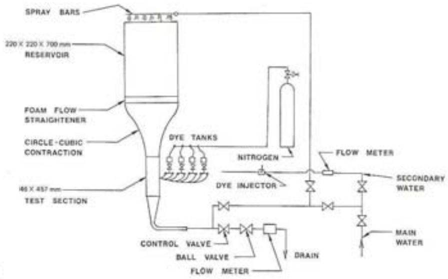

USAF/WAL pilot vertical water tunnel (US Air force Wright Aeronautical Lab, copied from *Fluid Mechanics Measurements*, Goldstein, 1983)

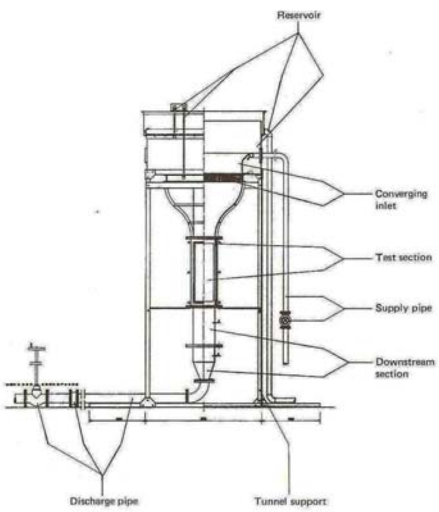

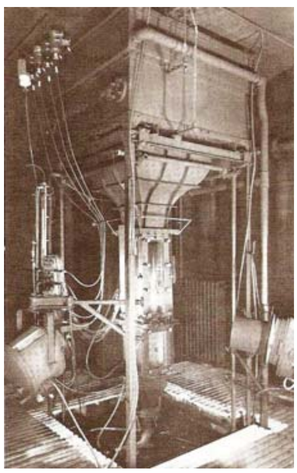

ONERA vertical water tunnel (Office National d'Etudes et de Recherches Aerospatiales, photocopied from *Fluid Mechanics Measurements*, Goldstein, 1983)

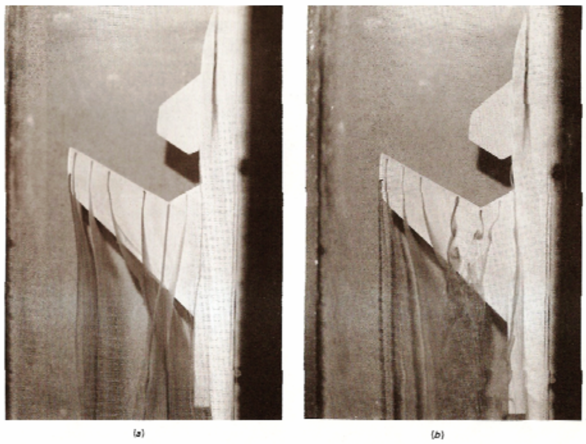

Figure 47 Forward-swept-wing model with canard at (a) $\alpha = 5°$ and $\beta = 2.5°$ and (b) $\alpha = 5°$ and $\beta - 5°$. (Courtesy of USAF/WAL.)

Continuous dye injection

- Hydrogen Bubble Method
  - Net reaction:

  $2H_2O \rightarrow 2H_2 + O_2$

  Anode reaction:

  $2H_2O \rightarrow O_2 + 4H^+ + 4e^-$

  Cathode reaction:

  $4H_2O + 4e^- \rightarrow 2H_2 + 4OH^-$

  - Buoyancy vs. drag
  - Both quantitative and qualitative

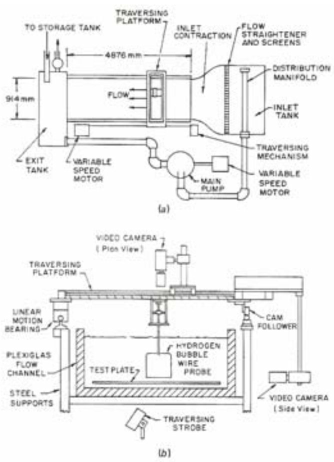

Figure 48 Lehigh University free-surface water channel. (a) Schematic of flow facility. (b) End-on view of channel (looking downstream) and traversing platform. (Courtesy of C. R. Smith and T. Wei, Lehigh University.)

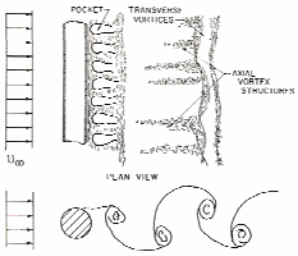

Figure 53 Sketch of the hydrogen-bubble patterns from the top and side of the circular cylinder. *(Courtesy of C. R. Smith and T. Wei, Lehigh Uni-*

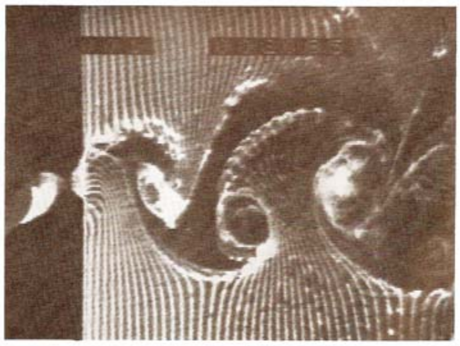

Figure 51 Photograph using a videographic copier of the periodic vortex-shedding pattern behind a circular cylinder. *(Courtesy of C. R. Smith and T. Wei, Lehigh University.)*

Hydrogen bubble
application

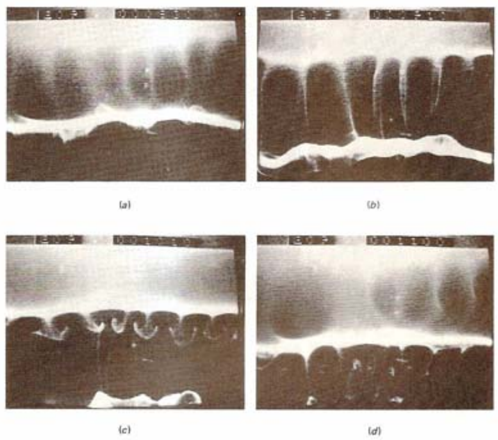

Figure 54 Hydrogen-bubble photographs from video monitor of the spanwise structure. (*a*) and (*b*) Formation of spanwise pockets. (*b*) and (*c*) Evolution to axial vortices. (*d*) Formation of a new set of spanwise pockets has just started. *(Courtesy of C. R. Smith and T. Wei, Lehigh University.)*

Hydrogen bubble
application

Figure 9.18 (p. 517) Flow visualization photographs of flow past an airfoil (the boundary layer velocity profiles for the points indicated are similar to those indicated in Fig. 9.17*b*): (*a*) zero angle of attack, no separation, (*b*) 5° angle of attack, flow separation. Dye in water. (Photograph courtesy of ONERA, France.)

(Copied from Munson et al., *Fundamentals of Fluid Mechanics*, 5th ed., 2005)

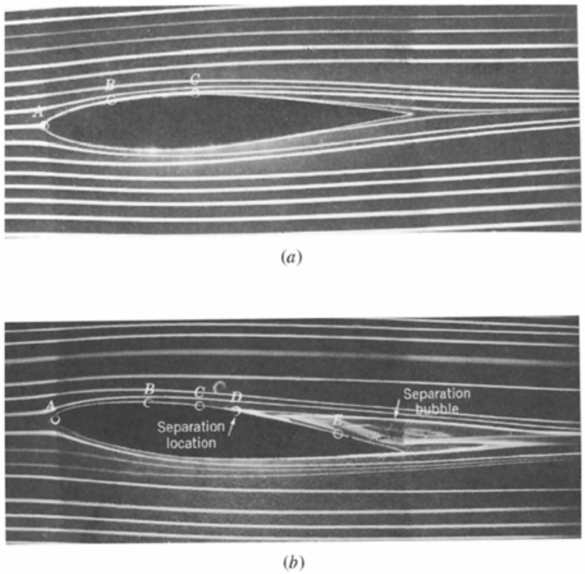

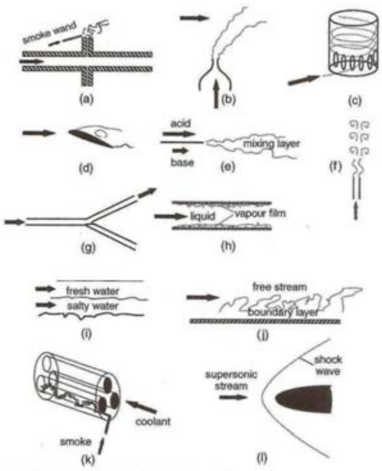

Figure 7.1. Examples of application of qualitative assessment techniques: (a) leakage detection, (b) detection of a draft or cross stream, (c) swirling flow pattern in a Diesel engine, (d) separation bubble over an airfoil, (e) mixing layer of reacting streams resulting in color change, (f) jet instability and break up, (g) flow direction in a fluidic switch, (h) steam–water flow in a heated tube, (i) density stratified flow, (j) turbulent boundary layer, (k) flow pulsations and coherent structures in gap regions of rod bundles, and (l) shock wave in supersonic flow over a bluff object.

Photocopied from Tavoularis (2005)

Optical Methods

- Direct visualization
  - Some type of marker (e.g., dye, bubbles, solid particles) is followed along with the fluid motion.
- Laser-Doppler systems
  - Frequency shift of scattered illumination from a marker is measured.
- Index-of-refraction (n) methods
  - Index of refraction or its spatial derivative of a medium is measured, from which some flow properties are determined.

23

- Index-of-refraction methods
  - Shadowgraph: 2nd derivative of $n \to d\rho^2/dx^2$
  - – For small effect of T variation, $n \sim 1$
  - Schlieren: 1st derivative of $n \to d\rho/dx$
  - Interferometer: $n \to \rho$
  - Advantages: nonintrusive, transient, various sensitivity of density for different problems and inferred properties …
  - Integral measurement, suited for 2D but …
  - Qualitative (for shadowgraph and schlieren), quantitative …

24

- Fundamentals
  - Lorentz-Lorentz relation for a homogeneous transparent medium $$\frac{1}{\rho}\frac{n^2-1}{n^2+1}=const$$
  - Gladstone-Dale equation when $n \approx 1$ $$\frac{n-1}{\rho}=C$$
    C: a function of the particular gas and varies slightly with λ
  - Using a standard condition $$n-1=\frac{\rho}{\rho_0}(n_0-1)$$
  - The derivatives are determined

$$\frac{\partial \rho}{\partial y}=\frac{1}{C}\frac{\partial n}{\partial y}=\frac{\rho_0}{n_0-1}\frac{\partial n}{\partial y}$$

$$\frac{\partial^2 \rho}{\partial y^2}=\frac{1}{C}\frac{\partial^2 n}{\partial y^2}=\frac{\rho_0}{n_0-1}\frac{\partial^2 n}{\partial y^2}$$

- For an ideal gas ($\rho = P/RT$) with constant pressure

$$\frac{\partial n}{\partial y}=-\frac{CP}{RT^2}\frac{\partial T}{\partial y}=-\frac{n_0-1}{T}\frac{\rho}{\rho_0}\frac{\partial T}{\partial y}$$

$$\frac{\partial T}{\partial y}=-\frac{T}{n_0-1}\frac{\rho}{\rho_0}\frac{\partial n}{\partial y}$$

$$\frac{\partial^2 n}{\partial y^2}=C\left[\frac{\rho}{T}\frac{\partial^2 T}{\partial y^2}+\frac{2\rho}{T^2}\left(\frac{\partial T}{\partial y}\right)^2\right]$$

- Using interferometer $$T=\frac{C}{n-1}\frac{P}{R}=\frac{n_0-1}{n-1}\frac{P}{P_0}T_0$$

- For a reversible, adiabatic (isentropic) process in an ideal gas

$$\frac{P}{P_0}=\left(\frac{n-1}{n_0-1}\right)^k$$

$$\frac{\partial P}{\partial y}=P\frac{k}{n-1}\frac{\partial n}{\partial y} \qquad \frac{\partial n}{\partial y}=\frac{1}{P}\frac{\partial P}{\partial y}\frac{n-1}{k}$$

- Schlieren system
  - Path of a light beam
  - – Variation of n in y direction
  - – Angular deflection of the ray

$$\Delta\alpha' \approx \frac{\Delta^2 z}{\Delta y} = -n\frac{\Delta(1/n)}{\Delta y}\Delta\tau\Delta y$$

In the limit $$d\alpha' = \frac{1}{n}\frac{\partial n}{\partial y}dz = \frac{\partial(\ln n)}{\partial y}dz$$

– For small deflection

$$\frac{\partial^2 y}{\partial z^2} = \frac{1}{n}\frac{\partial n}{\partial y}$$

$$\alpha' = \int \frac{1}{n}\frac{\partial n}{\partial y}dz = \int \frac{\partial(\ln n)}{\partial y}dz$$

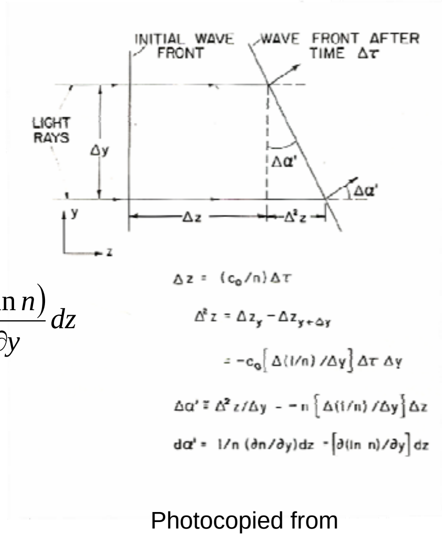

Photocopied from Goldstein (1983)

- For a test region enclosed by glass walls

Snell's law: $n_a \sin\alpha = n \sin\alpha'$, and for small angles

$$\alpha = \frac{n}{n_a}\int\frac{1}{n}\frac{\partial n}{\partial y}dz \approx \frac{1}{n_a}\int\frac{\partial n}{\partial y}dz \approx \int\frac{\partial n}{\partial y}dz$$

- For n with 2D variations in (x, y)

$$y'' = \frac{1}{n}\left[1+(x')^2+(y')^2\right]\left(\frac{\partial n}{\partial y} - y'\frac{\partial n}{\partial z}\right) \quad x'' = \frac{1}{n}\left[1+(x')^2+(y')^2\right]\left(\frac{\partial n}{\partial x} - x'\frac{\partial n}{\partial z}\right)$$

– The light beam turned toward increasing n and ρ (mostly)

– $\alpha \approx 10^{-6} - 10^{-3}$ rad

- Schlieren configuration

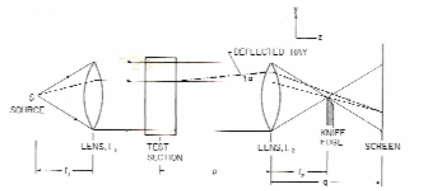

Figure 2 Typical schlieren system using lenses.

- Working principle of Schlieren technique

– Without disturbance

$$\frac{a_0}{a_s} = \frac{b_0}{b_s} = \frac{f_2}{f_1}$$

– Illumination with a knife edge $I_K = \frac{a_K}{a_0} I_0$

– After deflection

$$I_d = I_K \frac{a_K + \Delta a}{a_K} = I_K \left(1 + \frac{\Delta a}{a_K}\right)$$

Δa positive if the light is deflected away from the knife-edge; negative otherwise

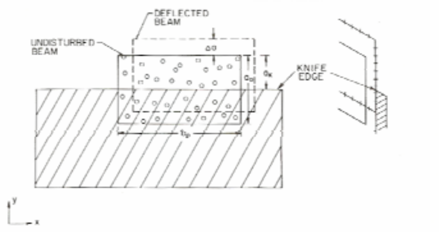

Figure 3 View of deflected and undisturbed beams at the knife-edge of a schlieren system.

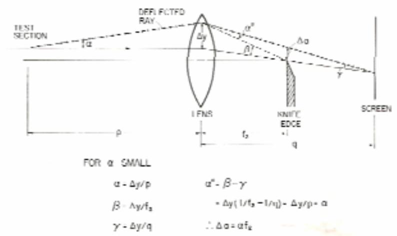

Figure 4 Ray displacement at knife-edge for a given angular deflection.

– Relative intensity or contrast

$$Contrast = \frac{\Delta I}{I_K} = \frac{I_d - I_K}{I_K} = \frac{\Delta a}{a_K} = \pm \frac{\alpha f_2}{a_K}$$

– Sensitivity for measuring the deflection

$$\frac{d(contrast)}{d\alpha} = \frac{f_2}{a_k}$$

$$Contrast = \frac{\Delta I}{I_K} = \pm \frac{f_2}{a_K n_a} \int \frac{\partial n}{\partial y} dz$$

– Assuming 2D field with constant $\partial n / \partial y$ at (x, y)

$$Contrast = \pm \frac{f_2}{a_K} \frac{1}{n_a} \frac{\partial n}{\partial y} L$$

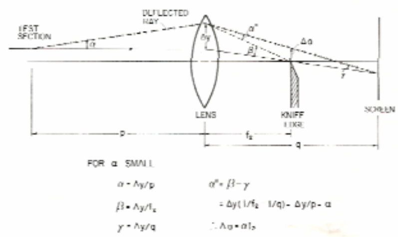

Figure 4 Ray displacement at knife-edge for a given angular deflection.

Photocopied from Goldstein (1983)

– For knife-edge covering $y < 0$; reversed otherwise

$$\frac{\Delta I}{I_K} = +\frac{f_2}{a_K}\frac{1}{n_a}\frac{\partial n}{\partial y}L$$

– For a gas

$$\frac{\Delta I}{I_K} = \pm\frac{f_2}{a_K n_a}\frac{n_0 - 1}{\rho_0}\int\frac{\partial\rho}{\partial y}dz$$

$$\approx \pm\frac{f_2}{a_K}\frac{n_0 - 1}{\rho_0}\frac{\partial\rho}{\partial y}L$$

For a gas at constant pressure

$$\frac{\Delta I}{I_K} = \mp\frac{f_2}{a_K n_a}\frac{n_0 - 1}{\rho_0}\int\frac{\rho}{T}\frac{\partial T}{\partial y}dz$$

– For a liquid

$$\frac{\Delta I}{I_K} = \pm\frac{f_2}{a_K n_a}\int\frac{\partial T}{\partial y}\frac{dn}{dT}dz$$

With 2D field

$$\frac{\Delta I}{I_K} = \pm\frac{f_2}{a_K n_a}\frac{\partial T}{\partial y}\frac{dn}{dT}L$$

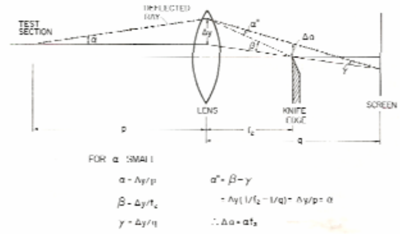

Figure 4 Ray displacement at knife-edge for a given angular deflection.

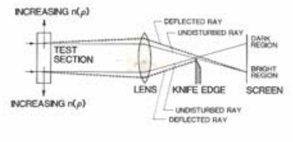

Photocopied from Goldstein (1983)

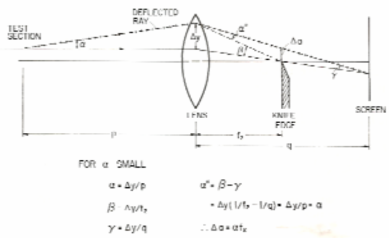

Figure 4 Ray displacement at knife-edge for a given angular deflection.

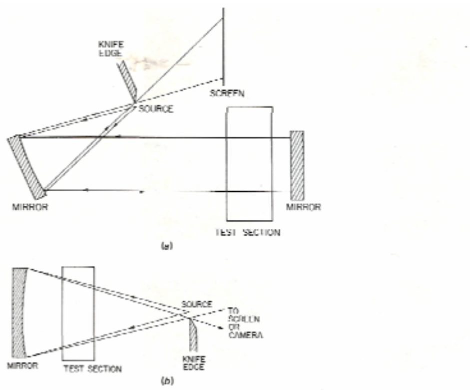

Figure 10 Alternative schlieren systems. (a) One converging and one plane mirror. (b) One converging mirror.

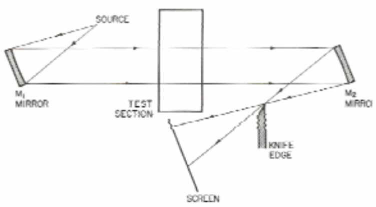

Figure 6 Typical schlieren system using converging mirrors.

Photocopied from Goldstein (1983)

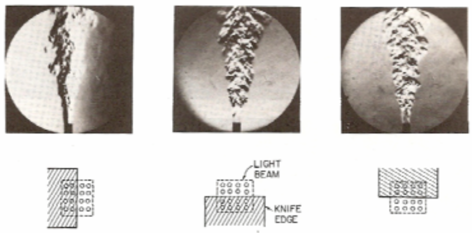

Figure 7 Schlieren images of a helium jet entering an atmosphere of air: The effect of knife-edge orientation (Re = 630).

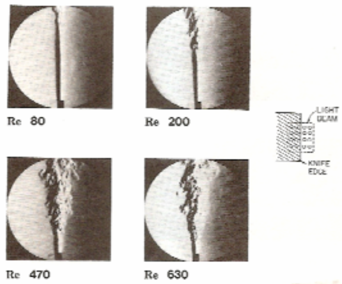

Figure 8 Schlieren images of the flow structure of a helium jet entering air at different Reynolds numbers.

Photocopied from Goldstein (1983)

33

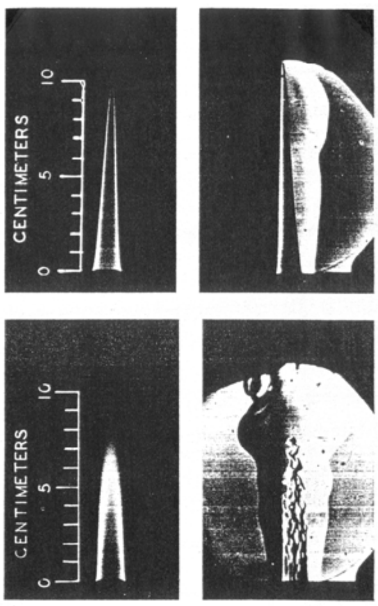

FIG. 215. Long-exposure (left) and instantaneous schlieren photograph (right) of a laminar and a turbulent flame. Upper part, laminar flow at Reynold number Re = 2000; lower part turbulent flow at Reynolds number Re = 3000. Stoichiometric mixture of natural gas and air. (Karlovitz et al.[2]).

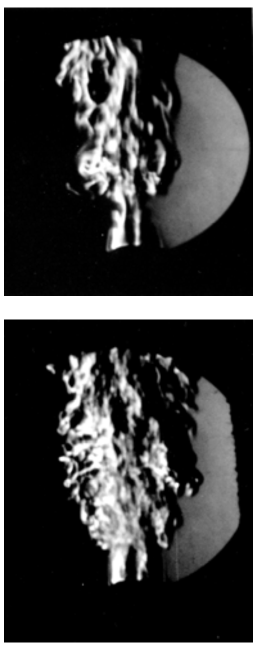

Pan, master thesis (1996)

- Shadowgraph system
  - Working principle

– Illumination

$$I_0 = \frac{\Delta y}{\Delta y_{SC}} I_T \qquad \Delta y_{SC} = \Delta y + z_{SC} d\alpha$$

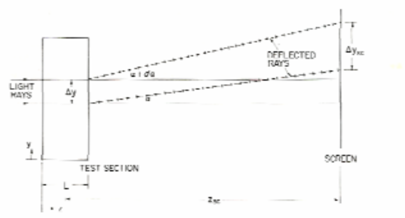

Figure 12 Displacement of light beam for shadowgraph evaluation.

– The contrast

$$\frac{\Delta I}{I_T} = \frac{I_0 - I_T}{I_T} = \frac{\Delta y}{\Delta y_{SC}} - 1 \approx -z_{SC}\frac{\partial \alpha}{\partial y} \qquad \rightarrow \frac{\Delta I}{I_T} = -\frac{z_{SC}}{n_a}\int \frac{\partial^2 n}{\partial y^2} dz$$

– For $n(\rho)$

$$\frac{\Delta I}{I_T} = -\frac{z_{SC}}{n_a}\int \frac{\partial^2 \rho}{\partial x^2}\cdot\frac{\partial n}{\partial \rho} dz$$

– 2D effect

$$\frac{\Delta I}{I_T} = -\frac{z_{SC}}{n_a}\int\left(\frac{\partial^2 n}{\partial x^2} + \frac{\partial^2 n}{\partial y^2}\right) dz$$

35

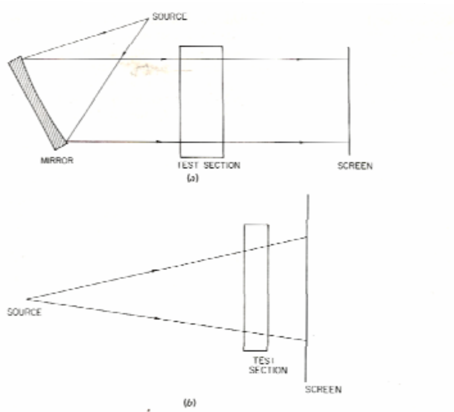

Figure 13 Alternative shadowgraph systems. (a) One converging mirror. (b) No lens or mirror.

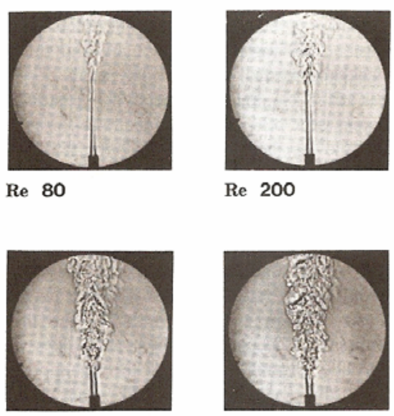

Photocopied from
Goldstein (1983)

36

- Interferometer
  - Often used for quantitative studies; not relied on deflection of a light beam; refraction effect usually of 2^{nd} order and undesired
  - *Mach-Zehnder interferometer*

– Large displacement of reference beam from test beam (once, sharp)

– Monochromatic light source

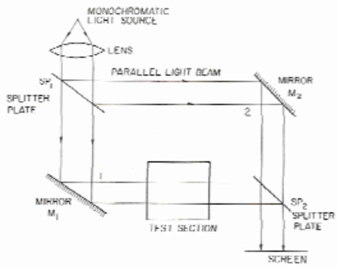

Figure 16 Mach-Zehnder interferometer.

Photocopied from Goldstein (1983)

- Working principle

– Amplitude of a plane light wave in a homogeneous medium

$$A = A_0 \sin \frac{2\pi}{\lambda}(c\tau - z)$$

– Combination of two waves

$$A_T = A_1 + A_2 = A_0\left[\sin\left(\frac{2\pi\ c\tau}{\lambda} - \Delta\right) + \sin\frac{2\pi\ c\tau}{\lambda}\right]$$

$$= 2A_0 \cos\frac{\Delta}{2}\sin\left(\frac{2\pi\ c\tau}{\lambda} - \theta\right)$$

– Light intensity I

– Optical path and phase difference $\quad PL = \int \frac{c_0}{c}dz = \lambda_0 \int \frac{dz}{\lambda}$

$$\overline{\Delta PL} = PL_1 - PL_2 = \lambda_0\left(\int_1 \frac{dz}{\lambda} - \int_2 \frac{dz}{\lambda}\right)$$

- Fringe pattern with Mach-Zehnder interferometer

– Path-length difference (neglecting refraction)

$$\varepsilon = \frac{\overline{\Delta PL}}{\lambda_0} = \frac{1}{\lambda_0}\int \left(n - n_{ref}\right)\, dz$$

$\rightarrow$ *fringes*: a series of bright and dark regions

– For 2D field $\qquad \varepsilon = \dfrac{n - n_{ref}}{\lambda_0} L$

– For a gas $\qquad \rho - \rho_{ref} = \dfrac{\lambda_0 \varepsilon}{CL} = \dfrac{\lambda_0 \varepsilon}{(n_0 - 1)L}\rho_0$

– For an ideal gas with constant pressure

$$\frac{1}{T} = \frac{\lambda_0 R}{PCL}\varepsilon + \frac{1}{T_{ref}} \qquad T = \frac{PCLT_{ref}}{PCL + \lambda_0 R\varepsilon T_{ref}}$$

$$T - T_{ref} = \left[\frac{-\varepsilon}{PCL/\left(\lambda_0 RT_{ref}\right) + \varepsilon}\right] T_{ref}$$

– For 2D field in a liquid

$$n = \frac{\lambda_0 \varepsilon}{L} + n_{ref}$$

– with small temperature differences

$$\varepsilon = \frac{L}{\lambda_0}\frac{dn}{dT}\left(T - T_{ref}\right) \qquad T - T_{ref} = \frac{\varepsilon\lambda_0}{L}\frac{1}{dn/dT}$$

E.g. $\lambda_0 = 546.1$ nm, $L = 30$ cm $\rightarrow$ each fringe: $\Delta T \approx 2$°C in air at 20 °C and 1 atm

- Fringe pattern

– Infinite fringe setting

– Wedge fringes

$$d = \frac{\lambda/2}{\sin\theta/2} \rightarrow d \sim \frac{\lambda}{\theta}$$

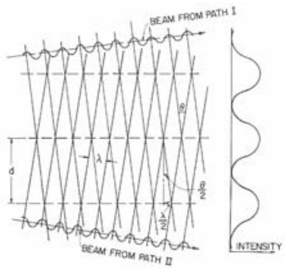

Photocopied from Goldstein (1983)

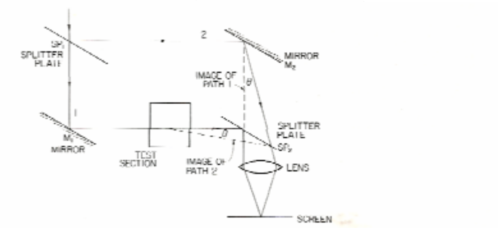

Figure 18 Light rays for Mach-Zehnder interferometer, indicating the preferred position of focus.

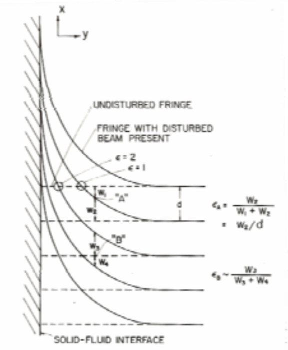

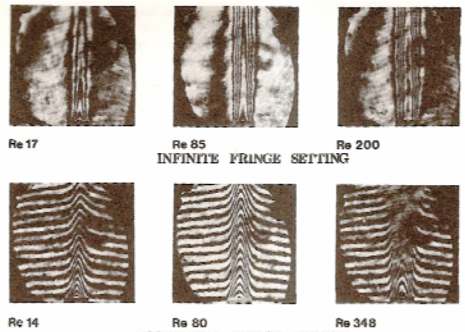

Figure 20 Interferograms of a low-Reynolds-number helium jet entering a still atmosphere of air.

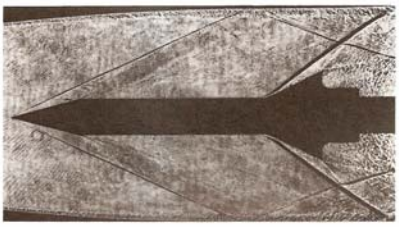

(a)

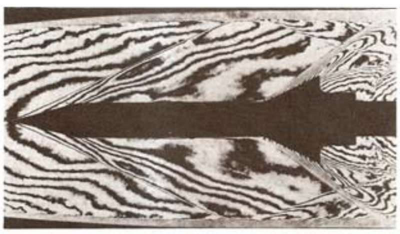

(b)

Figure 24 Flow over sharp-tipped spike with conical flare; pressure 100 psia; Ma = 2.98. (a) Shadowgraph. (b) Infinite-fringe interferogram. *(From [40].)*

(c)

Figure 24 Flow over sharp-tipped spike with conical flare; pressure 100 psia; Ma = 2.98. *(Continued)* (c) Wedge-fringe interferogram. *(From [40].)*

Photocopied from Goldstein (1983)

- Holography
  - Two beams are recombined on a photographic plate; resulted hologram: a diffraction grating formed by the emulsion on plate
  - If viewed from reference beam ~ Mach-Zehnder interferogram
    - 3D measurements of (ρ, T) possible
    - Low cost
    - Information from directions given by a single photograph (hologram)

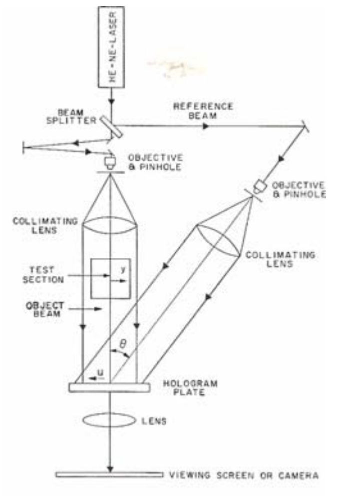

Photocopied from Goldstein (1983)

43

Flow Visualization Techniques Summary for Several Specific Cases

Marker methods	Measures	Fluid and speed
Dye or smoke	Displacement; qualitative	Low-speed flows
Surface powder	Displacement; qualitative	Open-surface liquid flow
Neutral density particles	Displacement; qualitative	Mainly liquids
Spark discharge	Displacement; qualitative	Low density gases
Hydrogen bubble	Displacement; quantitative	Electrolytic fluids
Aluminum flakes	Displacement; qualitative	Dense liquids
Photo-catalysis	Displacement; qualitative	
Electro-chemical luminescence	Velocity neat surfaces; qualitative	Low speed, special solutions

44

▪ Optical methods	Measures	Fluid and speed
• Shadowgraphy	$d^2\rho/dx^2$; quantitative	High-speed flows; or thermal or concentration gradients
• Schlieren system	$d\rho/dx$; quantitative	
• Interferometer	ρ; quantitative	
▪ Wall trace methods		
• Tufts • Evaporative and chemical change at wall	Velocity direction; transition; separation; reattachment	No basic limit
▪ Self-visible		
• Luminous	General motion; qualitative	Reacting/very high T
• Phase interfaces	Displacement of interface	Two-phase fluids

45